

Investigation of the magnetic hyperfine field at R and Zn sites in RZn (R=Gd, Tb, Dy) compounds using perturbed gamma-gamma angular correlation spectroscopy with ^{140}Ce and ^{111}Cd as probe nuclei

B. Bosch-Santos, A. W. Carbonari, G. A. Cabrera-Pasca, M. S. Costa, and R. N. Saxena

Citation: *Journal of Applied Physics* **113**, 17E136 (2013); doi: 10.1063/1.4798311

View online: <http://dx.doi.org/10.1063/1.4798311>

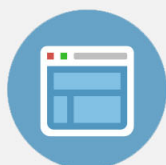
View Table of Contents: <http://scitation.aip.org/content/aip/journal/jap/113/17?ver=pdfcov>

Published by the [AIP Publishing](#)



Re-register for Table of Content Alerts

Create a profile.



Sign up today!



Investigation of the magnetic hyperfine field at R and Zn sites in RZn (R = Gd, Tb, Dy) compounds using perturbed gamma-gamma angular correlation spectroscopy with ^{140}Ce and ^{111}Cd as probe nuclei

B. Bosch-Santos, A. W. Carbonari,^{a)} G. A. Cabrera-Pasca, M. S. Costa, and R. N. Saxena
Instituto de Pesquisas Energéticas e Nucleares, University of São Paulo, São Paulo 05508-000, Brazil

(Presented 16 January 2013; received 5 November 2012; accepted 28 December 2012; published online 27 March 2013)

The magnetic hyperfine field (B_{hf}) in RZn compounds (R = Gd, Tb, Dy) has been investigated by perturbed angular correlation spectroscopy using ^{140}Ce and ^{111}Cd as probe nuclei, respectively, at R and Zn sites, in order to study the origin of the magnetic coupling in these compounds. The results for ^{111}Cd probe showed that the temperature dependence of B_{hf} roughly follows the Brillouin function for the R total angular momentum J of each compound. The temperature dependence of B_{hf} measured with ^{140}Ce probes showed, however, a sharp deviation from the Brillouin curve for all compounds, which was ascribed to the contribution of the 4f-electron of Ce^{3+} to B_{hf} . © 2013 American Institute of Physics. [<http://dx.doi.org/10.1063/1.4798311>]

I. INTRODUCTION

The study of magnetic properties of rare earth and zinc (RZn) compounds is interesting because the rare earth elements present a localized magnetism associated with 4f electrons, which do not participate in chemical bonds, and are responsible for the magnetic properties in these compounds. In this case, two different mechanisms have been proposed to explain the magnetic coupling between the 4f spins of rare-earth ions in the compound. One of them is the f - s mechanism wherein the s -conduction electrons mediate the 4f–4f coupling.¹ The other is the f – d mechanism in which the 5d electrons of the rare-earth ions is spin polarized by the inner 4f shell, and a subsequent 5d–5d exchange interaction with the 5d electrons of the neighboring rare-earth atoms comes about.^{2,3} In order to verify which of these two mechanisms is responsible for the magnetic coupling in RZn compounds, an investigation of the local magnetic field on an atomic scale is required.

The aim of the present work is to study the origin of the magnetic coupling in RZn (R = Gd, Tb, Dy) compounds. Perturbed gamma-gamma angular correlation (PAC) spectroscopy, which measures the hyperfine interaction between nuclear external fields and nuclear moments of the probe nuclei at a certain atomic site in the crystalline structure, was used in the present work to determine the experimental values of $B_{hf}(0)$ due to the coupling mechanism between 4f electrons of the R atoms in both R and Zn sites of GdZn, TbZn, and DyZn compounds. All compounds studied in this work exhibit a cubic crystal structure CsCl type belonging to space group $Pm\bar{3}m$. GdZn, TbZn, and DyZn compounds order ferromagnetically with Curie temperatures (T_C), respectively, 268, 204, and 139 K^{4,5} in which a tetragonal distortion was observed.

II. EXPERIMENTAL PROCEDURE

GdZn, TbZn, and DyZn samples were prepared by arc-melting the constituent elements (Gd, Tb, Dy = 99.9% and Zn = 99.999% purity) in stoichiometric proportions under argon atmosphere purified with a hot titanium getter. The structure of samples was characterized by X-ray diffraction, whose results for GdZn and DyZn showed a single phase corresponding to the CsCl structure. In the case of TbZn, the results showed that a major fraction (~73%) of the sample presents the expected CsCl structure, while a minor fraction (~27%) presents the hexagonal structure of the metal Tb. These two phases were previously observed in TbZn as reported in the literature.⁶

PAC measurements were carried out in a four BaF₂ detector spectrometer using ^{140}La (^{140}Ce) and ^{111}In (^{111}Cd) nuclear probes. For the measurements with ^{111}In (^{111}Cd) nuclear probes, a carrier free ^{111}In in the form of $^{111}\text{InCl}_3$ was thermally diffused into the samples at 800 °C for 6 h, 700 °C for 8 h, and 500 °C for 10 h, respectively, for GdZn, TbZn, and DyZn. Radioactive ^{140}La was introduced in the sample by arc melting the constituent elements of the compounds along with ~0.1% of La previously irradiated with neutrons. After melting, samples were annealed in vacuum at 800 °C for 6 h, 750 °C for 12 h, and 470 °C during 32 h, respectively, for GdZn, TbZn, and DyZn. The gamma cascades of 171–245 keV in ^{111}Cd populated in the electron capture decay of ^{111}In and 329–487 keV in ^{140}Ce populated from the decay of ^{140}Ce were used for the PAC measurements, which were carried out in the temperature range of 10–295 K using a closed loop helium cryogenic system. A detailed description of the experimental method can be found elsewhere.^{7,8}

III. RESULTS AND DISCUSSION

Results of PAC measurements with ^{111}Cd for DyZn were fitted with a model described by a single fraction with a

^{a)}Electronic mail: carbonar@ipen.br

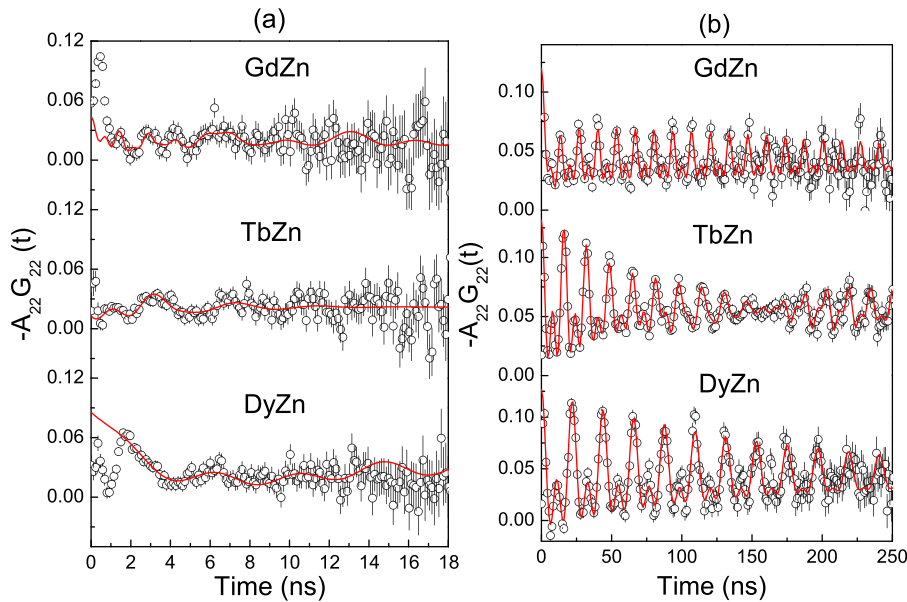


FIG. 1. Perturbation functions for RZn measured with (a) ^{140}Ce at 50 K and (b) ^{111}Cd at 10 K. Solid lines are the least squares fit of the theoretical functions to the experimental data.

well-defined magnetic frequency, which was assigned to probe nuclei substituting the regular position of Zn atom in the cubic structure. Results for GdZn and TbZn were fitted using two fraction sites for probe nuclei, with the major fraction ($\sim 65\%$) being assigned to probe nuclei replacing Zn sites and the minor fraction with a broadly distributed frequency for GdZn and a well defined fraction for TbZn assigned to probe nuclei replacing Tb position in the hexagonal crystal structure of Tb. The PAC spectra for RZn measured with ^{140}Ce at indicated temperatures are shown in Fig. 1(a) and the results of measurements with ^{111}Cd at indicated temperatures are shown in Fig. 1(b).

Fig. 2 shows the temperature dependence of the magnetic hyperfine field B_{hf} measured with ^{140}Ce (a) and ^{111}Cd (b). For each compound, the B_{hf} could be calculated from the measured Larmor frequency (ω_L) using the relation $\omega_L = \mu_N g B_{hf} / \hbar$, where μ_N is the nuclear magneton and g is the g -factor of the intermediate level of each probe nucleus, which, for ^{111}Cd and ^{140}Ce , are, respectively, 0.306 ± 0.001 and 1.014 ± 0.038 .¹⁰

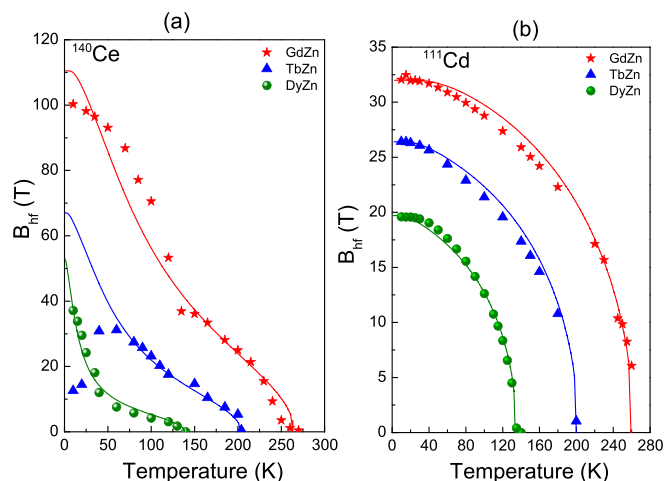


FIG. 2. Temperature dependence of the magnetic field for RZn measured with (a) ^{140}Ce and (b) ^{111}Cd probe nuclei.

The use of ^{140}Ce probe is interesting to study local magnetism because this probe nucleus has a small electric quadrupole moment that makes it practically insensitive to electric quadrupole interactions, being sensitive only to magnetic dipole interactions. It is, therefore, useful to define quite accurately the temperature of the magnetic transitions as well as the magnetic hyperfine field at the rare-earth positions. The temperature dependence of B_{hf} measured with ^{140}Ce for each studied compound is shown in Fig. 2(a). A sharp deviation of the experimental values from the Brillouin curve can be observed for each compound. This deviation results from the presence of one $4f$ electron in the Ce^{+3} ion, which may contribute to the total hyperfine field.⁹ A similar deviation was recently observed in RRh_2Si_2 ($\text{R} = \text{rare-earth element}$) compounds.¹¹ The origin of this contribution to the observed B_{hf} at ^{140}Ce probes was explained by the relative position of the $4f$ band of the Ce impurity in the density of states for each compound, and we believe that the same mechanism is responsible by the temperature dependence behavior of B_{hf} in the studied RZn compounds. The $4f$ band of the Ce impurity is located near the Fermi level, hybridized with the $4d$ bands which are wide and extend above the Fermi level. As the polarization of the $4f$ band of the impurity by the $4f$ electrons of the rare-earth element of the host occurs via d band, when temperature increases, more d -electrons are promoted to energies above the Fermi level weakening the polarization of the Ce $4f$ -band, resulting in a decrease in B_{hf} values.¹¹

One can thus consider the effective B_{hf} at ^{140}Ce on rare-earth positions as a sum of the host contribution (B_{hf}^h) plus a contribution from the impurity Ce (B_{hf}^i), $B_{hf} = B_{hf}^h + B_{hf}^i$. A model based on the molecular field theory modified to be used with rare-earth host and impurity^{12,13} was used to obtain these two contributions. Results of the fit are shown in Fig. 2(a) as solid lines. Data points at low temperature for TbZn were not included in the fit once they represent a possible decrease in B_{hf} due to the presence of a non-magnetic state of Ce probe ion.¹⁴ We, so far, do not know the reason why data at low temperature deviate from the fit in the case

TABLE I. Results for the fit of Brillouin function to experimental B_{hf} data measured with ^{111}Cd in RZn compounds. B_{hf} measured with ^{111}Cd in R elements¹⁵ and ratio $B_{hf}(RZn)/B_{hf}(R)$ are also displayed.

Compound	T_C (K)	$B_{hf}(0)$ (T)	Element	$B_{hf}(0)$ (T)	$\frac{B_{hf}(RZn)}{B_{hf}(R)}$
GdZn	261(1)	32.0(8)	Gd	-34.0(7)	0.94(3)
TbZn	202(1)	26.4(6)	Tb	-27.5(5)	0.96(3)
DyZn	135(1)	19.7(5)	Dy	-22.1(4)	0.89(3)

of GdZn. However, as this effect is caused by the probe itself and the host contribution follows a Brillouin like behavior as shown in Fig. 2(b), we have considered that these effects do not appreciably change the host contribution to B_{hf} .

The results for the behavior of B_{hf} with temperature measured with ^{111}Cd (Fig. 2(b)), which measured only the host contribution, could be reasonably fitted using the Brillouin function for the total angular momentum (J) of each rare-earth ion: $J_{Gd} = 7/2$, $J_{Tb} = 6$, $J_{Dy} = 15/2$, respectively, for GdZn, TbZn, and DyZn. From this fit, the magnetic field at 0 K [$B_{hf}(0)$] and the Curie temperature (T_C) could be obtained. Results are shown in Table I.

Both coupling mechanisms described in introduction result in spin polarization which, through Fermi contact interaction, produces a magnetic hyperfine field at the probe nucleus. One, therefore, expects B_{hf} to be linearly proportional to spin projection of S along J , $(g-1)J$.¹⁶ Results of B_{hf} at 0 K obtained from the fit for both probe nuclei, ^{111}Cd and ^{140}Ce (host contribution), show linear dependence with $(g-1)J$.

In order to investigate the coupling mechanism, we have followed the same procedure described in Ref. 15 and compared B_{hf} measured with ^{111}Cd in RZn to that in rare-earth elements (R). In RZn, ^{111}Cd probes have 8 nearest R neighbors at Zn sites, while in R metals each site has 12 NN. In the $f-d$ mechanism, we, therefore, expect that the ratio $B_{hf}(RZn)/B_{hf}(R) \sim 8/12 = 0.67$ or larger. In the case of $f-s$ mechanism, $B_{hf}(RZn)$ is roughly 0.5 of the $B_{hf}(R)$, because half of the R ions are replaced by Zn atoms. In Table I, B_{hf} measured with ^{111}Cd for rare-earth elements $R = \text{Gd, Tb, and Dy}$ as well as the ratio $B_{hf}(RZn)/B_{hf}(R)$ are displayed. As can be seen from the results, $B_{hf}(RZn)/B_{hf}(R)$ are all larger than 0.67 which is a good indication that the $f-d$ mechanism is responsible for the magnetic coupling in these compounds.

IV. SUMMARY

PAC spectroscopy using ^{140}Ce and ^{111}Cd was used to measure the temperature dependence of B_{hf} , respectively, at

R and Zn sites in RZn ($R = \text{Gd, Tb, Dy}$) compounds. Results for ^{111}Cd could be fitted by the Brillouin function, which allowed determination of the Curie temperature as well as B_{hf} at 0 K. Although B_{hf} values for ^{140}Ce strongly depart from the Brillouin behavior because the $4f$ -electron contribution to B_{hf} , the host contribution could be determined from the fit of a molecular-field based model. The host contribution to B_{hf} follows a linear dependence with $g_J - 1$ for two probe nuclei, and a comparison of B_{hf} values for RZn with those for R measured with ^{111}Cd indicated that the $f-d$ mechanism may be responsible for the spin coupling in these compounds.

ACKNOWLEDGMENTS

Partial financial support for this research was provided by Fundação de Amparo a Pesquisa no Estado de São Paulo (FAPESP). B.B.S., A.W.C., and R.N.S. thankfully acknowledge the support provided by CNPq. M.S.C. thankfully acknowledges the support provide by CAPES.

¹M. A. Ruderman and C. Kittel, *Phys. Rev.* **96**, 99–102 (1954); T. Kasuya, *Prog. Theor. Phys.* **16**, 45–57 (1956); K. Yosida, *Phys. Rev.* **106**, 893–898 (1957).

²S. Blundell, *Magnetism in Condensed Matter* (Department of Physics, University of Oxford, 2001).

³D. Torumba, V. Vanhoof, M. Rots, and S. Cottenier, *Phys. Rev. B* **74**, 014409 (2006).

⁴K. H. J. Buschow, *Rep. Prog. Phys.* **42**, 1373–1477 (1979).

⁵P. Morin, J. Rouchy, and E. Du Tremolet de Lacheisserie, *Phys. Rev. B* **16**, 3182–3193 (1977).

⁶D. W. Delaney and T. A. Lograsso, *J. Magn. Magn. Mater.* **205**, 311–318 (1999).

⁷R. Dogra, A. C. Junqueira, R. N. Saxena, A. W. Carbonari, J. Mestnik-Filho, and M. Morales, *Phys. Rev. B* **63**, 224104 (2001).

⁸A. W. Carbonari, R. N. Saxena, W. Pendl, Jr., J. Mestnik-Filho, R. N. Atilli, M. Olzon-Dionysio, and S. D. de Souza, *J. Magn. Magn. Mater.* **163**, 313–321 (1996).

⁹A. W. Carbonari, J. Mestnik-Filho, R. N. Saxena, and M. V. Lalic, *Phys. Rev. B* **69**, 144425 (2004).

¹⁰R. M. Levy and D. A. Shirley, “Hyperfine structure in the 2084 keV State of ^{140}Ce ,” *Phys. Rev.* **140**, B811–815 (1965).

¹¹G. A. Cabrera-Pasca, A. W. Carbonari, B. Bosch-Santos, J. Mestnik-Filho, and R. N. Saxena, *J. Phys.: Condens. Matter* **24**, 416002 (2012).

¹²A. W. Carbonari, F. H. M. Cavalcante, L. F. D. Pereira, G. A. Cabrera-Pasca, J. Mestnik-Filho, and R. N. Saxena, *J. Magn. Magn. Mater.* **320**, e478–e480 (2008).

¹³G. A. Cabrera-Pasca, A. W. Carbonari, R. N. Saxena, B. Bosch-Santos, J. A. H. Coaquira, and J. A. Filho, *J. Alloys Compd.* **515**, 44–48 (2012).

¹⁴T. A. Thiel, E. Gerdau, B. Scharnberg, and M. Böttcher, *Hyperfine Interact.* **14**, 347–362 (1983).

¹⁵M. Forker, R. Mubeler, and S. C. Bedi, *Phys. Rev. B* **71**, 094404 (2005).

¹⁶S. Müller, P. de La Presa, and M. Forker, *Hyperfine Interact.* **158**, 163–167 (2004).